Biodistribution of the Fatty Acid Analogue ^{18}F-FTHA: Plasma and Tissue Partitioning Between Lipid Pools During Fasting and Hyperinsulinemia

Letizia Guiducci[1–3], Tove Grönroos[1], Mikko J. Järvisalo[1], Jan Kiss[1,4], Antti Viljanen[1], Alexandru G. Naum[1], Tapio Viljanen[1], Timo Savunen[4], Juhani Knuuti[1], Ele Ferrannini[3,5], Piero A. Salvadori[3], Pirjo Nuutila[1,6], and Patricia Iozzo[1,3]

[1]Turku PET Centre, University of Turku, Turku, Finland; [2]Medical Sciences Branch, SSSUP, Pisa, Italy; [3]PET Centre, Institute of Clinical Physiology, CNR National Research Council, Pisa, Italy; [4]Department of Surgery, University of Turku, Turku, Finland; [5]Department of Internal Medicine, University of Pisa School of Medicine, Pisa, Italy; and [6]Department of Medicine, University of Turku, Turku, Finland

Alterations of free fatty acid (FA) metabolism in several organs are implicated in the pathogenesis of chronic disorders. The aim of this study was to investigate the biodistribution and partitioning of the FA analog, 14(*R,S*)-^{18}F-fluoro-6-thia-heptadecanoic acid (^{18}F-FTHA), across different lipid pools in plasma and in metabolically important organs and its response to insulin. **Methods:** Eight anesthetized pigs were studied during fasting or euglycemic insulin stimulation. Plasma samples from the carotid artery, hepatic vein, and portal vein were collected at 10 and 40 min after ^{18}F-FTHA injection via indwelling catheters. The animals were then sacrificed and tissue biopsies rapidly obtained from the heart, brain, liver, subcutaneous and visceral fat, pancreas, intestine, and skeletal muscle. Radioactivity was assessed in the FA, phospholipid, and triglyceride or glycerol ester pools. **Results:** The tissue-to-plasma intact ^{18}F-FTHA ratio was high in all tissues, with the highest values being in the heart and liver; ^{18}F-FTHA accumulated in the brain to a significant extent. Hyperinsulinemia was associated with higher plasma ^{18}F-FTHA clearance ($P < 0.05$) and lower labeled triglyceride appearance ($P \leq 0.01$) than those associated with fasting, indicating faster tissue removal and suppressed hepatic triglyceride release. Tracer retention was enhanced in skeletal muscle, pancreas, and visceral fat ($P < 0.05$ vs. fasting). Under both study conditions, tissue radioactivity was greatly accounted for by glycerol ester. **Conclusion:** ^{18}F-FTHA is a promising tracer in PET imaging of metabolically important organs, which are currently inaccessible in vivo. Physiologic hyperinsulinemia enhances plasma tracer clearance in fat, skeletal muscle, and pancreas.

Key Words: ^{18}F-FTHA; insulin; fatty acid metabolism; brain; PET

J Nucl Med 2007; 48:455–462

Free fatty acids (FAs) are high-energy compounds and a main fuel of human tissues (*1*). Their energy can be stored in the form of glycerol esters within all body organs, and they are rapidly mobilized from adipose tissue and liver back to the circulation as free FA or triglycerides, respectively, to meet the energy requirements of the organism (*2*). Regional dysregulation of FA metabolism—involving high levels of FAs and triglycerides in blood and in normally lean organs—is implicated in the pathogenesis of some primary chronic disorders such as diabetes, cardiovascular disease, cancer, and obesity (*3,4*). In this context, several body organs are involved at different levels. Thus, adipose tissue lipolysis and triglyceride release from the liver, together with regional FA uptake and storage in various organs, control plasma lipid levels. In the brain, the signaling role of FA is increasingly implicated in the modulation of peripheral metabolism (*5*), but the in vivo characterization of this regulatory interaction is challenging, and the use of ^{11}C-palmitate and PET in the quantification of brain FA uptake has proven cumbersome, given the rapid clearance of the tracer from this organ (*6*). Pancreatic FA exposure and its influence on insulin secretion, which is the most important hormonal signal regulating FA metabolism in the rest of the body, is another field of intensive and growing investigation, lacking a satisfactory methodology (*7*).

We and others have previously used the FA analog 14(*R,S*)-^{18}F-fluoro-6-thia-heptadecanoic acid (^{18}F-FTHA) and PET to quantify regional FA metabolism, especially in the myocardium and skeletal muscle. ^{18}F-FTHA is a false long-chain FA that is taken up by tissues to enter mitochondria or be incorporated into complex lipids (*8*). In mitochondria, ^{18}F-FTHA undergoes the initial steps of β-oxidation and is then trapped because further β-oxidation is blocked by its sulfur heteroatom (*9*). Because of this property, ^{18}F-FTHA has provided optimal target-to-background signal on PET images in the investigated organs. The biodistribution and partitioning of ^{18}F-FTHA between different lipid

Received Aug. 28, 2006; revision accepted Dec. 3, 2006.

For correspondence or reprints contact: Patricia Iozzo, MD, PhD, Turku PET Centre, P.O. Box 52, University of Turku, Turku, Finland.
E-mail: patricia.iozzo@ifc.cnr.it

pools in plasma and body tissues have been poorly characterized, and no studies are available on the metabolic fate of ^{18}F-FTHA in the brain, adipose tissue, and pancreas, which are primary metabolic regulatory organs. The existing ex vivo information is mostly limited to the heart, skeletal muscle, and liver and has been derived mainly from small animals (*8,10*), but extrapolation from rodents to humans requires great caution. The influence of nutritional changes is also relevant, because the inability of tissues to switch their substrate use away from FA breakdown under insulin stimulation is regarded as a main mechanism in disease pathogenesis. Besides, the ex vivo evaluation of the tissue-to-blood input tracer ratio is instrumental in defining the suitability of a tracer for quantitative PET.

The present study was performed to characterize the biodistribution of ^{18}F-FTHA and its partitioning between the FA, phospholipid, and triglyceride or glycerol ester pools in plasma and in metabolically active body tissues (heart, brain, liver, subcutaneous and visceral fat, pancreas, intestine, and skeletal muscle) during fasting and insulin-stimulated conditions. The study was conducted on pigs, the animal model most translational to humans.

MATERIALS AND METHODS

Animal Experiments

Anesthetized animals were studied during fasting ($n = 4$) or euglycemic hyperinsulinemia ($n = 4$). The protocol was reviewed and approved by the Ethical Committee for Animal Experiments of the University of Turku. After an approximately 16-h fasting period, the pigs (body weight range, 28–31 kg) were anesthetized with ketamine and pancuronium and were mechanically ventilated via tracheal intubation with oxygen and normal room air (regulated ventilation, 16 breaths per minute). Catheters were placed in the jugular vein, carotid artery, and femoral vein for the administration of glucose, insulin, and ^{18}F-FTHA and for the sampling of arterial blood. Splanchnic vessels were accessed by a subcostal incision. After dissection of the hepatogastric ligament, purse string sutures were allocated to allow catheter insertion in the hepatic and portal veins via a small incision. Doppler flow probes were placed around the portal vein. The surgical access site was closed, and distal catheter extremities were secured to the abdominal surface to avoid tip displacement. Vital signs, blood pressure, and heart rate were monitored throughout the study. ^{18}F-FTHA was produced as previously described (*11*) and was administered (321 ± 50 MBq) by a rapid intravenous injection. In the hyperinsulinemic studies (*12*), an intravenous prime-continuous insulin infusion (5 $mU \cdot kg^{-1} \cdot min^{-1}$) was performed. During hyperinsulinemia, euglycemia was maintained by a 10% dextrose infusion. The rate of dextrose infusion was adjusted according to the results of frequent monitoring of plasma glucose concentration. The tracer was injected during steady state.

Blood samples were simultaneously collected at 10 and 40 min after ^{18}F-FTHA injection from catheters placed into the left carotid artery, the portal vein, and the hepatic vein. Blood samples were collected in dry syringes, transferred in ethylenediaminetetraacetic acid–coated tubes, mixed, and immediately stored in ice until the analytic procedures could be performed. Additional blood samples were withdrawn from the carotid artery to determine total plasma radioactivity concentrations. Unlabeled free FA and triglyceride levels were measured at the beginning and end of studies, using previously described procedures (*13*).

At 1 h after injection, the animals were sacrificed through an injection of potassium chloride and an overdose of anesthetic, and tissue biopsy samples of the heart, brain, liver, subcutaneous and visceral fat, pancreas, intestine, and skeletal muscle were rapidly collected and processed. Some data on plasma palmitate kinetics in parts of these animals have previously been reported (*14*).

Extraction and Counting of Labeled Lipid Fractions from Plasma and Tissue

Blood samples were centrifuged at 5°C (5 min, 3,000 rpm), and 0.5 mL of plasma was separated, transferred into a clean tube, and mixed with 2 mL of extraction solution (Dole reagent [a 1:10:40 mixture of 1N HCl:n-heptane:2-propanol]) (*15*). After stirring of the samples in a vortex mixer (30 s), 2 mL of water and 1.5 mL of heptane were added, the samples were mixed (30 s) and centrifuged (4 min at 4,000 rpm), and the organic phase was transferred into a collecting vial with a Pasteur glass pipette. Then, 1.5 mL of n-heptane were added to the remaining phase, and samples were mixed for 30 s and centrifuged at 4,000 rpm for 4 min to separate and count the residual aqueous phase. The organic phase was again transferred to the collecting vial and was sequentially eluted at positive pressure through an activated solid-phase extraction column (SPE-NH_2; International Sorbent Technology Ltd.) to separate lipid fractions. The triglyceride fraction was collected first, by elution with 3 mL of heptane/isopropanol (1:2), followed by free FA and phospholipid, which were collected by elution with 4 mL of 2% acetic acid in diethyl ether and 4 mL of MeOH, respectively. Radioactivity in each fraction was measured in a well counter (7.62 × 7.62 cm, NaI crystal, 3Mw3/3P; Bicron Inc.).

Lipids were extracted from tissues using a previously described method (*16*). Tissue samples were weighed, homogenized in 2 mL of MeOH, and centrifuged (5 min at 5,000 rpm). The upper phase (supernatant) was transferred to an Eppendorf tube and centrifuged again (5 min at 5,000 rpm). Then, 1 mL of sample solution was added to 2 mL of chloroform, mixed, diluted in 2 mL of water, and again mixed and centrifuged (5 min, 5,000 rpm). The supernatant (watery phase) was separated and counted. The lower organic phase was collected up to the protein disk using a Pasteur pipette. Glycerol ester, free FA, and phospholipid were separated by SPE-NH_2 columns and counted, as described above. The method here adopted to separate the water from the organic fraction has recently been implemented by others (*10*), who have documented, via use of standards, that the organic fraction so derived contains the above-listed species and a small amount of cholesteryl ester. The latter was not specifically measured in this study, and it may account for a less than 5% overestimation in other fractions. We conducted classic spike experiments in which ^{18}F-FTHA was added to unlabeled tissue and plasma samples, showing that 5%–15% of radioactivity was recovered in other than the FA fraction; this range is not much different from what is seen with natural FA tracers (5%–10%).

Calculations

The metabolite-corrected arterial time–activity curve was used for the determination of ^{18}F-FTHA clearance (mL/min) by dividing the injected dose (kBq) by the area under the radioactivity curve (time 0 to infinity) (kBq·min/mL). Tracer balance (percentage of injected dose, or %ID/min) across the extrahepatic

splanchnic compartment was calculated as the product of the arterial–portal venous difference and portal blood flow; tracer balance across the liver was calculated as the difference between tracer influx (i.e., arterial and portal radioactivity levels multiplied by respective blood flow) and outflux (as product of hepatic venous radioactivity levels and hepatic blood flow); the contribution of portal to hepatic perfusion was considered to be 83%—as determined in previous studies conducted under similar conditions (*17,18*)—and was used to estimate arterial and total hepatic blood flow. Radioactivity levels in tissues at 60 min after injection were divided by the area under the curve of the metabolite-corrected liver input function (0–60 min) to obtain a retention index. Partitioning of the tracer between FA, glycerol ester or triglyceride, phospholipid, and hydrophilic pools in tissue and plasma samples was expressed as radioactivity in 1 g of tissue (or 1 mL of plasma) divided by the injected dose × 100 (%ID/g or %ID/mL).

Statistical Analysis

All data are expressed as mean ± SEM. The Student paired *t* test or ANOVA, as appropriate, was used in group comparisons. Statistical analyses were performed using the StatView software package. A *P* value of less than 0.05 was considered statistically significant.

RESULTS

Metabolic Characteristics

The characteristics of the study animals, including blood substrate concentrations, are presented in Table 1 and show that the 2 study groups were well matched at baseline. During hyperinsulinemia, serum free FA and triglyceride concentrations decreased by 90% and by more than 70%, respectively, from baseline ($P < 0.03$) and were significantly lower ($P \leq 0.05$) than in the fasting state.

Plasma ^{18}F-FTHA Biodistribution

The amount of intact ^{18}F-FTHA in samples obtained from arterial blood and portal and hepatic veins showed a significant decrease in radioactivity concentrations from 10 to 40 min after injection under both fasting conditions (artery, $P = 0.05$; hepatic vein, $P < 0.01$; portal vein, $P = 0.06$) and hyperinsulinemic conditions (artery, $P = 0.04$; portal vein, $P = 0.05$) (Fig. 1). At 10 min, plasma levels of intact ^{18}F-FTHA were lower in hyperinsulinemic experiments than in fasting experiments, indicating faster tissue removal during the first minutes after injection. This difference was partially compensated for by a more rapid decline between 10 and 40 min in the fasting state, as shown in Figure 1. As a result, the overall calculated tracer clearance (from time 0 to infinity) showed higher values during hyperinsulinemia (1,993 ± 117 vs. 1,342 ± 123 mL/min, $P = 0.01$), implying that the initial clearance is numerically more relevant (Fig. 2). ^{18}F-Labeled triglycerides (Fig. 1) were already detectable at 10 min after ^{18}F-FTHA injection under both fasting and euglycemic hyperinsulinemic conditions, with no significant difference between the conditions at this time point. At 40 min, they were significantly increased in all 3 vessels and under both conditions but to a largely different extent, with a 9-fold rise at 40 versus 10 min in the fasting state (artery, $P = 0.0056$; hepatic vein, $P = 0.0058$; portal vein, $P = 0.0125$) and a 3-fold rise during hyperinsulinemia (artery, $P = 0.0165$; hepatic vein, $P = 0.0256$; portal vein, $P = 0.0054$). Consequently, at 40 min after tracer injection, labeled triglycerides were significantly higher during fasting than during hyperinsulinemia ($P \leq 0.01$ in all vessels) (Fig. 1), representing 53% ± 5% and 18% ± 2% of overall arterial plasma radioactivity,

TABLE 1
Metabolic Characteristics of the Study Animals

Characteristic	Fasting (n = 4)	Hyperinsulinemia (n = 4)	P
Body weight (kg)	30.6 ± 0.7	31.0 ± 0.4	NS
Before injection/insulin infusion			
P-glucose (mmol·l^{-1})	7.1 ± 0.7	6.0 ± 0.6	NS
P-lactate (mmol·l^{-1})	4.2 ± 1.3	3.2 ± 0.9	NS
S-cholesterol (mmol·l^{-1})	1.6 ± 0.1	1.7 ± 0.1	NS
S-TG-artery (mmol·l^{-1})	0.475 ± 0.048	0.400 ± 0.041	NS
S-free FA-artery (mmol·l^{-1})	0.137 ± 0.017	0.186 ± 0.032	NS
S-TG-hepatic vein (mmol·l^{-1})	0.450 ± 0.065	0.350 ± 0.065	NS
S-free FA-hepatic vein (mmol·l^{-1})	0.082 ± 0.006	0.230 ± 0.088	0.02
S-TG-portal vein (mmol·l^{-1})	0.425 ± 0.063	0.375 ± 0.063	NS
S-free FA-portal vein (mmol·l^{-1})	0.141 ± 0.015	0.189 ± 0.028	NS
At steady state during clamping/fasting			
S-TG-artery (mmol·l^{-1})	0.450 ± 0.019	0.150 ± 0.050	0.05
S-free FA-artery (mmol·l^{-1})	0.276 ± 0.050	0.030 ± 0.008	0.028
S-TG-hepatic vein (mmol·l^{-1})	0.400 ± 0.265	0.100 ± 0.00	NS
S-free FA-hepatic vein (mmol·l^{-1})	0.279 ± 0.083	0.026 ± 0.004	0.013
S-TG-portal vein (mmol·l^{-1})	0.600 ± 0.100	0.125 ± 0.025	0.003
S-free FA-portal vein (mmol·l^{-1})	0.377 ± 0.093	0.031 ± 0.004	0.01

NS = not statistically significant; P = plasma; S = serum; TG = triglyceride.
Data are mean ± SEM.

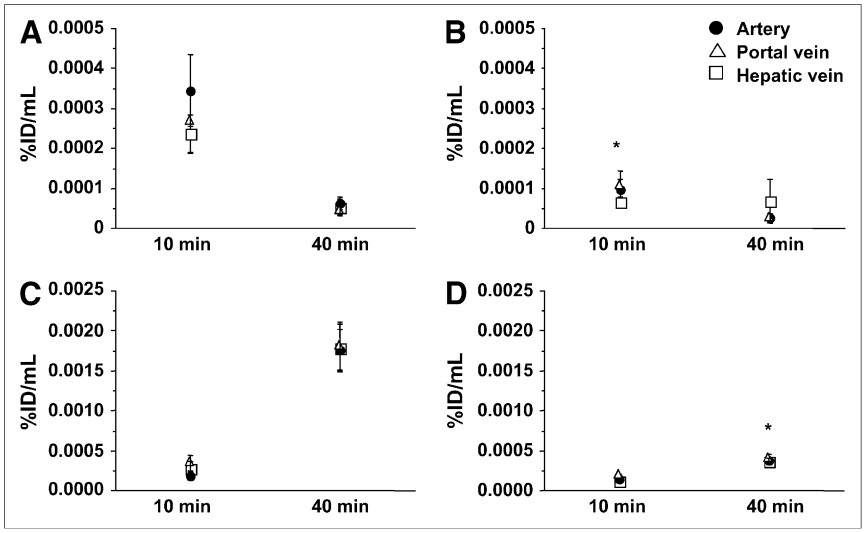

FIGURE 1. Plasma levels of unchanged ^{18}F-FTHA (A and B) and ^{18}F-FTHA–labeled triglyceride (C and D) in 3 vessels at 10 and 40 min during fasting (A and C) and hyperinsulinemic (B and D) studies. Lower levels of ^{18}F-FTHA at 10 min after injection suggest that, during hyperinsulinemia, there is a rapid early clearance that is partially compensated for by a more rapid decline between 10 and 40 min during the fasting state. The SEM in ^{18}F-FTHA levels during hyperinsulinemia at 40 min was due to a single outlying value, elevating the group average. $^*P < 0.05$ vs. respective fasting values.

respectively. A high proportion of hydrophilic radioactivity (fasting, 79% ± 3%, vs. hyperinsulinemia, 90% ± 1%; $P = 0.006$) was recovered in plasma at 10 min after injection. At 40 min, hydrophilic radioactivity remained relatively higher under hyperinsulinemic conditions than under fasting conditions (44 ± 5 vs. 80% ± 2%, $P = 0.0007$), possibly reflecting more rapid ^{18}F-FTHA metabolism during hyperinsulinemia.

Tissue ^{18}F-FTHA Biodistribution

Radioactivity levels (%ID/g) in the heart and liver were approximately twice those in the other tissues (Table 2); consistently, the balance of ^{18}F-FTHA across the liver was positive under both conditions (0.05–0.06 %ID/min = 3–3.6 %ID in the whole liver over 60 min). Though evaluation of tissue uptake by arterial–venous differences at single time points after bolus injection is influenced by the transit time of the labeled substrate across the organ (*19*), data on liver radioactivity showed values of approximately 0.003–0.0034 %ID/g (Table 2), corresponding to 3–3.4 %ID in the average 1-kg liver. These values are similar to those obtained above from the organ balance. Radioactivity levels did not vary between fasting and hyperinsulinemia in most organs, with the exception of an insulin-induced 100% increase in visceral adipose tissue ($P = 0.028$ vs. fasting) and an approximately 20%–50% reduction in the explored brain regions ($P = 0.1$) (statistically significant at $P = 0.015$ after exclusion of a single outlying value). When data were expressed as retention index, thus accounting for circulating ^{18}F-FTHA, that is, the plasma input to tissue, hyperinsulinemia was associated with significantly higher tracer uptake rates in skeletal muscle and pancreas, besides visceral fat ($P < 0.05$ vs. fasting) (Fig. 3). The tissue-to-plasma input radioactivity ratio ranged from 7.3 to 93.9 during fasting and from 26.4 to 236.2 during hyperinsulinemia; it was lowest in the skeletal muscle and highest in the heart, with intermediate values being observed in brain regions (Table 3).

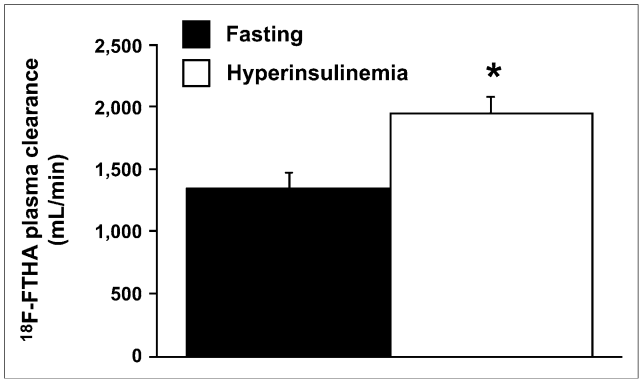

FIGURE 2. Calculated overall (time 0 to infinity) tracer clearance showing significant insulin-mediated increase. This variable cumulates the effects observed in Figure 1, showing that early clearance has a numerically more important impact on the overall process. $^*P = 0.01$ vs. fasting state.

Under both study conditions and in all tissues, radioactivity was largely accounted for by glycerol ester, with a 5%–10% or lower fraction in FA and phospholipid and the remainder in the aqueous phase (Table 2). In the myocardium, skeletal muscle, and subcutaneous fat, the aqueous-to-glycerol ester ratio was more than 1.0, whereas most of the label was found in the glycerol ester pool in most other tissues, with minimum aqueous-to-glycerol ester ratios in the brain. There were no significant differences in the amount of tracer recovered in glycerol ester between the 2 study conditions, but again, when the input function was taken into account, a significantly higher amount of labeled glycerol ester was observed in subcutaneous and visceral adipose tissue in the hyperinsulinemic group ($P = 0.004$ and $P = 0.01$ vs. fasting, respectively) (Fig. 3). The tissue response to insulin in terms of ^{18}F-FTHA recovery in individual lipid fractions, especially glycerol ester, agreed somewhat with global tissue radioactivity. The only exception

TABLE 2
Tissue Biodistribution of ^{18}F-FTHA

Tissue type	Total radioactivity	Glycerol esters	FTHA unchanged	Hydrophilic phase
Fasting				
Liver	3.425 ± 1.465	2.105 ± 0.994	0.123 ± 0.053	0.804 ± 0.288
Visceral fat	0.771 ± 0.189	0.438 ± 0.145	0.025 ± 0.005	0.270 ± 0.102
Subcutaneous fat	0.480 ± 0.147	0.162 ± 0.052	0.036 ± 0.017	0.259 ± 0.106
Pancreas	0.936 ± 0.394	0.578 ± 0.341	0.047 ± 0.016	0.229 ± 0.087
Intestine	1.308 ± 0.227	0.606 ± 0.162	0.046 ± 0.004	0.548 ± 0.132
Skeletal muscle	0.419 ± 0.069	0.183 ± 0.069	0.012 ± 0.003	0.201 ± 0.048
Heart	5.404 ± 1.075	2.624 ± 0.901	0.052 ± 0.021	2.632 ± 0.175
Cerebellum	1.049 ± 0.389	0.682 ± 0.321	0.049 ± 0.009	0.255 ± 0.055
Brain cortex	0.932 ± 0.422	0.599 ± 0.311	0.058 ± 0.016	0.218 ± 0.080
Corpus callosum	1.345 ± 0.469	0.968 ± 0.449	0.088 ± 0.012	0.211 ± 0.072
Hyperinsulinemia				
Liver	3.065 ± 0.500	1.331 ± 0.212	0.082 ± 0.014	1.259 ± 0.297
Visceral fat	1.513 ± 0.178*	0.825 ± 0.167	0.036 ± 0.007	0.571 ± 0.079*
Subcutaneous fat	0.557 ± 0.041	0.242 ± 0.022	0.012 ± 0.007	0.283 ± 0.031
Pancreas	1.307 ± 0.089	0.631 ± 0.083	0.065 ± 0.013	0.469 ± 0.036*
Intestine	1.317 ± 0.116	0.599 ± 0.054	0.078 ± 0.020	0.496 ± 0.023
Skeletal muscle	0.482 ± 0.034	0.237 ± 0.032	0.010 ± 0.007	0.222 ± 0.016
Heart	4.766 ± 0.612	1.862 ± 0.268	0.052 ± 0.011	2.723 ± 0.458
Cerebellum	0.801 ± 0.302†	0.367 ± 0.196	0.027 ± 0.009	0.308 ± 0.091
Brain cortex	0.665 ± 0.151†	0.371 ± 0.099	0.032 ± 0.011	0.227 ± 0.046
Corpus callosum	0.716 ± 0.118†	0.489 ± 0.049	0.046 ± 0.022	0.184 ± 0.063

Data are expressed as %ID/g × 10^3 (*$P < 0.05$ and †$P \leq 0.1$ vs. fasting).

was the pancreas, in which the increase in global radioactivity was accounted for by enhanced metabolism as documented by a higher tracer fraction in the hydrophilic phase. The balance of labeled triglyceride across the extrahepatic splanchnic compartment (including intestine, pancreas, and visceral fat) was negative under both study conditions (−0.03 %ID/min).

DISCUSSION

To the best of our knowledge, this was the first study detailing the tissue and plasma biodistribution of the FA analog ^{18}F-FTHA under fasting and insulin-stimulated conditions in a large-animal model that translates to humans reliably. Our data revealed tissue-specific regulation of the fate of the tracer by nutritional state, together with rapid stimulation of its plasma clearance and suppression of ^{18}F-labeled triglyceride release by insulin.

One important finding was that the organ-to-plasma input radioactivity ratio was much greater than 1 in all study organs. A high tissue signal with respect to the tracer input is a fundamental requirement in PET quantification, by allowing separation of the time–activity curve in the tissue of interest from that in vessels. Good heart and liver image quality has been known for some time (*20,21*); the present results indicated that ^{18}F-FTHA holds promise in the quantitative imaging of a series of metabolically relevant organs. In particular, ^{18}F-FTHA may be suitable for brain studies; in our animals, the brain tissue-to-input ratio was approximately 17 to 37 (fasting-to-insulin), suggesting that ^{18}F-FTHA crosses the blood–brain barrier and accumulates persistently and measurably.

The current results revealed pronounced differences in tissue handling of ^{18}F-FTHA. Because data were expressed per unit of tissue mass, the myocardium was significantly more avid in extracting FAs than were the other organs, and

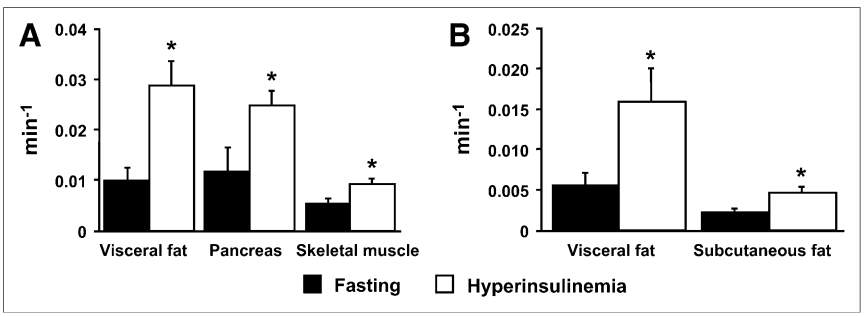

FIGURE 3. Retention index, as calculated from total (A) and glycerol ester (B) tissue radioactivity. *$P < 0.05$ vs. fasting.

TABLE 3
Tissue-to-Plasma Input Radioactivity Ratio

Tissue type	Fasting	Hyperinsulinemia	*P*
Liver	52.6 ± 21.9	138.8 ± 21.8	0.03
Visceral fat	12.8 ± 3.4	86.2 ± 29.8	0.06
Subcutaneous fat	8.5 ± 3.3	29.8 ± 8.7	0.05
Pancreas	13.1 ± 3.7	71.9 ± 22.7	0.04
Intestine	22.9 ± 4.7	67.6 ± 17.9	0.05
Skeletal muscle	7.3 ± 1.2	26.4 ± 8.4	0.06
Heart	93.9 ± 41.6	236.2 ± 59.4	0.12
Cerebellum	15.8 ± 3.5	47.5 ± 26.8	0.28
Cortex	13.4 ± 3.9	30.9 ± 7.1	0.07
Corpus callosum	21.2 ± 5.5	33.7 ± 8.8	0.27

Input is represented by intact ^{18}F-FTHA radioactivity levels in arterial plasma in all organs, with exception of liver, in which combined contribution of portal venous and arterial input concentrations was used.

its label was distributed predominantly to the hydrophilic and glycerol ester phases, indicating active breakdown and storage consistent with the high energy requirements of this tissue. The proportion of activity found in the myocardial hydrophilic phase (~50%) was somewhat lower than that described in our previous investigation on mitochondria (89%) (*11*). Notably, this study was conducted 60 min after injection, as opposed to 30 min in the previous study. Thus, more time was allowed for some potential escape of labeled metabolites because the myocardial ^{18}F clearance half-time has been shown to be around 2 h in ^{18}F-FTHA studies (*8*). More important, partitioning of FA in the heart varies with workload, as recently demonstrated (*22*); in our previous study, animals had undergone sternotomy, with pericardial access for catheter placement in the atrium and coronary sinus, which may account for a different workload. In addition, the activity measured in mitochondria (34%) had been divided by the organelle yield (31%–46%) to obtain the full ^{18}F mitochondrial fraction, introducing some degree of overestimation as documented by values in excess of 100%. Overall, our current and previous ^{18}F-FTHA data are in line with the observation (*22*) that roughly half of FAs are conveyed to glycerol ester under normal conditions, a proportion that is considerably reduced in favor of the oxidative pathway during increased workload.

Extrapolating the current dataset to the whole organism, with adipose tissue and skeletal muscle typically corresponding to 25% and 40%, respectively, of body weight, and with an average liver weight of 1 kg, the overall clearance of ^{18}F-FTHA was accounted for mostly by adipose tissue, liver, and skeletal muscle, in that order. Overall, the liver may handle more ^{18}F-FTHA than may skeletal muscle despite the smaller (<1/10) tissue mass of the liver. This possibility is in accord with our previous observations in human ^{18}F-FTHA PET studies (*23*) and would confirm the central role of the organ in regulating whole-body FA exposure.

The response to insulin stimulation varied among tissues. By normalizing tissue radioactivity concentrations to the injected dose, as is customarily done in ex vivo biodistribution studies, hyperinsulinemia was associated with a slight increase in tracer retention in most organs and with a proportional change in each lipid fraction, which did not achieve statistical significance except in visceral fat. Importantly, the use of the plasma input function improved the interpretation of our data by accounting for the effective concentrations of tracer available for organ extraction and their changes during hyperinsulinemia. As a result, pronounced upregulation of ^{18}F-FTHA uptake was observed in adipose tissue, skeletal muscle, and pancreas. In the former, this upregulation was associated with a higher incorporation of label in glycerol ester. Normally, hyperinsulinemia is induced by meal ingestion to promote substrate storage in view of the subsequent fasting period. In general, insulin suppresses endogenous FA release in any form (*24*), thus reducing the uptake of endogenous FA. This effect is counterbalanced by the introduction of exogenous lipids with the meal, and—as demonstrated here—by a direct action of the hormone in enhancement of ^{18}F-FTHA uptake and incorporation into glycerol ester in fat depots. The fact that skeletal muscle is a large organ with high energy requirements may explain the preservation of an inner reservoir of FA suggested by our results. The pancreas is responsible for adjusting insulin secretion to the metabolic needs of the organism, thus producing the postprandial insulin rise to allow proper handling of nutrients. The evidence that hyperinsulinemia promoted ^{18}F-FTHA uptake by this organ suggests that FA serves as an insulin-mediated signal, regulating hormonal control in a feedback fashion. Clearly, the plasticity shown by these organs in rapidly adapting to an acute metabolic stimulus indicates that even a modest reduction in their flexibility, such as is described in obesity, may have whole-body repercussions. The remarkable amount of FAs handled by the liver and heart, together with the dramatic change in triglyceride release by the former after insulin stimulation, supports their cause–effect involvement in disease pathogenesis. In agreement with our current findings, the myocardial fractional extraction of ^{18}F-FTHA did not change under pharmacologic insulin stimulation in rats (*10*) or physiologic hyperinsulinemia in humans (*13*), and the hormonal effect of decreasing FA uptake was mediated by the suppression of circulating endogenous FFA levels. Other studies have shown that the competitive action of lactate oversupply on substrate oxidative pathways decreased the extraction fraction of ^{18}F-FTHA (*25*), therefore suggesting that the fractional extraction of ^{18}F-FTHA correlates with FA uptake in this organ; these findings can hardly be extrapolated to the current experiments. Different from the purely competitive mechanism of lactate overflow, insulin is secreted to promote tissue energy storage, besides glucose oxidation, and the complexity of its action in redistributing substrate resources involves local and systemic mechanisms, as well as oxidative and storage enzymes.

Notably, extrapolation of ^{18}F-FTHA data to endogenous FA metabolism must account for differences in the properties of this tracer from those of native FA. In rodents, a recent evaluation has highlighted qualitative differences between the oxidative and nonoxidative partitioning of ^{18}F-FTHA and ^{14}C-palmitate despite similar tissue uptake rates and insulin responses in the heart and skeletal muscle (*10*). Though liver metabolism differs greatly across species, the comparison between our current data and previous plasma ^{11}C-palmitate data in the pig (*14*) seems to extend to large animals the evidence of a limited affinity of ^{18}F-FTHA for triglyceride shown in rodents (*10*). Most thia-FAs are substrates of the mitochondrial carrier and can be conveyed into the organelle. In particular, the 6-thia-FA used here can undergo 2 cycles of β-oxidation and is presumably metabolized to an 8-^{18}F-undecanethiol and its unknown protein-bound metabolites (*8*), which are presumably recovered as hydrophilic radioactivity. This property of the tracer accounts for its slow mitochondrial clearance, such that ^{18}F-metabolites are retained in gross proportion to ^{18}F-FTHA entrance into mitochondria, as opposed to natural FAs, which are cleared from tissue as β-oxidation occurs. In contrast, though the bulk of radioactivity in the organic phase is recovered from glycerol ester (*10*), unlike natural FAs, ^{18}F-FTHA seems to be a better substrate for diacyl- than triacyl-glycerol esters. The subsequent metabolism may be affected because of steric or charge hindrance, preventing the conversion of diglycerides into triglycerides (*10*), and could result in a lower hepatic release of triglyceride synthesized from plasma FA. A lower affinity of ^{18}F-FTHA for triglyceride synthesis partly explains the lack of repartitioning of the tracer from the hydrophilic to the glycerol ester pool during hyperinsulinemia, although the effects of insulin on these processes are incompletely understood. These features are relevant in the interpretation of the external signal obtained during PET, in which tracer retention may variably be related to mitochondrial or glycerol ester activity, and the specificity of the signal is dependent on the organ and the nutritional or pharmacologic stimulus under investigation. The biodistribution analysis performed here is meant to support the future interpretation of PET data obtained under the conditions of the current investigation.

The signaling of FAs to central nuclei has been involved in the regulation of liver glucose output (*5*) and pancreatic insulin secretion (*26*) and in the control of food intake and energy expenditure. These regulatory processes are difficult to address in humans in vivo, and most data in this regard have been demonstrated in small animals by intracerebroventricular FA administration (*27*). Our study is contributory by revealing that ^{18}F-FTHA may be a suitable tracer in human brain studies. Given the limited sample size in the current investigation, the effects of insulin on brain ^{18}F-FTHA retention did not achieve statistical significance; however, the demonstration that the tracer reaches the brain, and the description of its intracellular distribution, may support a broader evaluation in humans to better delineate the hormonal action.

The evaluation of plasma ^{18}F-FTHA kinetics documented that labeled triglycerides were already measurable in plasma 10 min after label injection, indicating hepatic uptake of ^{18}F-FTHA and synthesis of complex lipids and their release into the bloodstream. In the fasting state, triglyceride release increased rapidly and progressively, by 9-fold on average, within a 30-min sampling interval, reflecting the continuous involvement of the liver in triglyceride-associated FA provision to peripheral tissues. This process persisted but lessened by two thirds during insulin stimulation; these findings are consistent with the role of insulin in promoting FA storage after meal ingestion and they may be explained somewhat by a lower availability of ^{18}F-FTHA during hyperinsulinemia (*28*). In fact, at 10 min from the start of the experiments, both circulating ^{18}F-FTHA levels and circulating FA levels were significantly lower in hyperinsulinemic than fasting animals, suggesting higher FA clearance, which typically could not be counterbalanced by adipose tissue lipolysis because of the suppressive effect of insulin on this process. The quantification of ^{18}F-FTHA clearance documented an insulin-mediated 50% increase, in agreement with our previous evidence using carbon-labeled palmitate (*14*); this change was almost fully explained by a consensual change in adipose tissue storage of labeled glycerol ester, as indicated by the organ biodistribution data. Though ^{18}F-FTHA clearance was higher, and labeled triglyceride levels lower, than those obtained with carbon-labeled palmitate, insulin-induced modifications in plasma kinetics were similar in relative magnitude, direction, and statistical significance. A relevant fraction of label appeared as hydrophilic radioactivity in plasma, probably reflecting, to some extent, mitochondrial breakdown products. All in all, plasma ^{18}F-FTHA kinetics suggest that insulin accelerates whole-body uptake and storage of FA while suppressing endogenous FA oxidation and FA and triglyceride output from adipose tissue and liver, respectively.

CONCLUSION

Our data indicate that ^{18}F-FTHA is a suitable tracer for quantitative PET of metabolically important organs and is sensitive to changes in tissue and plasma between fasting and insulin stimulation, though, given the limited sample size, broader in vivo studies will more powerfully delineate the hormonal action. The interpretation of ^{18}F-FTHA data has to account for the specific properties of the analog, only partially reflecting the fate of native FAs. The use of a plasma input function, as opposed to the injected-dose normalization, was instrumental in the interpretation of tissue biodistribution results.

ACKNOWLEDGMENTS

This work was part of the project "Hepatic and Adipose Tissue and Functions in the Metabolic Syndrome"

(HEPADIP; http://www.hepadip.org/), which is supported by the European Commission as an Integrated Project under the 6th Framework Programme (contract LSHM-CT-2005-018734). The study was further supported by grant 206359 from the Academy of Finland; grant QKGA-1999-51330 from the MCTS program; a fellowship from EFSD/Eli-Lilly; and grants from the Finnish Diabetes Foundation, the Sigrid Juselius Foundation, and the Novo Nordisk Foundation. We are grateful to the technical staff of the Turku PET Centre for the effort and skill that they dedicated to this project.

REFERENCES

1. Mittendorfer B, Liem O, Patterson BW, Miles JM, Klein S. What does the measurement of whole-body fatty acid rate of appearance in plasma by using a fatty acid tracer really mean? *Diabetes.* 2003;52:1641–1648.
2. Aarsland A, Chinkes D, Wolfe RR. Contributions of de novo synthesis of fatty acids to total VLDL-triglyceride secretion during prolonged hyperglycemia/hyperinsulinaemia in normal man. *J Clin Invest.* 1996;98:2008–2017.
3. Boden G, Shulman GI. Free fatty acids in obesity and type 2 diabetes: defining their role in the development of insulin resistance and β-cell dysfunction. *Eur J Clin Invest.* 2002;32(suppl 3):14–23.
4. Knuuti J, Takala TO, Nagren K, et al. Myocardial fatty acid oxidation in patients with impaired glucose tolerance. *Diabetologia.* 2001;44:184–187.
5. Pocai A, Obici S, Schwartz GJ, Rossetti L. A brain-liver circuit regulates glucose homeostasis. *Cell Metab.* 2005;1:53–61.
6. Arai T, Wakabayashi S, Channing MA, et al. Incorporation of [1-carbon-11]palmitate in monkey brain using PET. *J Nucl Med.* 1995;36:2261–2267.
7. Lupi R, Del Guerra S, Fierabracci V, et al. Lipotoxicity in human pancreatic islets and the protective effect of metformin. *Diabetes.* 2002;51:S134–S137.
8. DeGrado TR, Coenen HH, Stocklin G. 14(R,S)-[^{18}F]Fluoro-6-thia-heptadecanoic acid (FTHA): evaluation in mouse of new probe of myocardial utilization of long chain fatty acid. *J Nucl Med.* 1991;32:1888–1896.
9. DeGrado TR, Wang S, Holden JE, Nickles J, Taylor M, Stone C. Synthesis and preliminary evaluation of 18 F-labeled 4-thia palmitate as a PET tracer of myocardial fatty acid oxidation. *Nucl Med Biol.* 2000;27;3:221–231.
10. Ci X, Frisch F, Lavoie F, et al. The effect of insulin on the intracellular distribution of 14(R,S)-[^{18}F]fluoro-6-thia-heptadecanoic acid in rats. *Mol Imaging Biol.* 2006;8:237–244.
11. Takala TO, Nuutila P, Pulkki K, et al. 14(R,S)-[^{18}F]fluoro-6-thia-heptadecanoic acid as a tracer of free fatty acid uptake and oxidation in myocardium and skeletal muscle. *Eur J Nucl Med Mol Imaging.* 2002;29:1617–1622.
12. DeFronzo RA, Tobin JD, Andres R. Glucose clamp technique: a method for quantifying insulin secretion and resistance. *Am J Physiol.* 1979;237:E214–E223.
13. Mäki MT, Haaparanta M, Nuutila P, et al. Free fatty acid uptake in the myocardium and skeletal muscle using fluorine-18-fluoro-6-thia-heptadecanoic acid. *J Nucl Med.* 1998;39:1320–1327.
14. Guiducci L, Järvisalo M, Kiss J, et al. ^{11}C-Palmitate kinetics across the splanchnic bed in arterial, portal and hepatic venous plasma during fasting and euglycaemic hyperinsulinaemia. *Nucl Med Biol.* 2006;33:521–528.
15. Dole VP. A relation between non-esterified fatty acid in plasma and metabolism of glucose. *J Clin Invest.* 1956;35:150–154.
16. Nemeth PM, Hitchinns OE, Solanki L, Cole TG. Fluorometric procedures for measuring triglyceride concentrations in small amounts of tissue and plasma. *J Lipid Res.* 1986;27:447–452.
17. Iozzo P, Jarvisalo MJ, Kiss J, et al. Quantification of liver glucose metabolism by positron emission tomography: validation study in pigs. *Gastroenterology.* 2007;132. In press.
18. DeFronzo RA. Use of the splanchnic/hepatic balance technique in the study of glucose metabolism. *Baillieres Clin Endocrinol Metab.* 1987;1:837–862.
19. Zierler K. Theory of the use of arteriovenous concentration differences for measuring metabolism in steady and non-steady states. *J Clin Invest.* 1961;40:2111–2125.
20. Takala TO, Nuutila P, Katoh C, et al. Myocardial blood flow, oxygen consumption, and fatty acid uptake in endurance athletes during insulin stimulation. *Am J Physiol.* 1999;277:E585–E590.
21. Iozzo P, Turpeinen AK, Takala T, et al. Liver uptake of free fatty acids in vivo in humans as determined with 14(R, S)-[^{18}F]fluoro-6-thia-heptadecanoic acid and PET. *Eur J Nucl Med Mol Imaging.* 2003;30:1160–1164.
22. Stowe KA, Burgess SC, Merritt M, Sherry AD, Malloy CR. Storage and oxidation of long-chain fatty acids in the C57/BL6 mouse heart as measured by NMR spectroscopy. *FEBS Lett.* 2006;580:4282–4287.
23. Iozzo P, Turpeinen AK, Takala T, et al. Defective liver disposal of free fatty acids in patients with impaired glucose tolerance. *J Clin Endocrinol Metab.* 2004;89:3496–3502.
24. Carpentier A, Frisch F, Cyr D, et al. On the suppression of plasma non-esterified fatty acid by insulin during enhanced intravascular lipolysis in humans. *Am J Physiol Endocrinol Metab.* 2005;289:E849–E856.
25. Stone CK, Pooley RA, DeGrado TR, et al. Myocardial uptake of the fatty acid analog 14-fluorine-18-fluoro-6-thia-heptadecanoic acid in comparison to beta-oxidation rates by tritiated palmitate. *J Nucl Med.* 1998;39:1690–1696.
26. Tirone TA, Brunicardi FC. Overview of glucose regulation. *World J Surg.* 2001;25:461–467.
27. Kreier F, KapYS, Mettenleiter TC, et al. Tracing from fat tissue, liver, and pancreas: a neuroanatomical framework for the role of the brain in type 2 diabetes. *Endocrinology.* 2006;147:1140–1147.
28. Shumak SL, Zinman B, Zuniga-Guarjardo S, Poapst M, Steiner G. Triglyceride-rich lipoprotein metabolism during acute hyperinsulinaemia in hypertriglyceridemic humans. *Metabolism.* 1988;37:461–466.